



The contact heat transfer between the heating plate and granular materials in rotary heat exchanger under overloaded condition

Luanfang Duan, Chonggang Qi, Xiang Ling*, Hao Peng*

Jiangsu Key Laboratory of Process Enhancement and New Energy Equipment Technology, School of Mechanical and Power Engineering, Nanjing Tech University, No. 30 Pu Zhu South Road, Nanjing 211816, PR China



ARTICLE INFO

Article history:

Received 10 July 2017

Received in revised form 1 November 2017

Accepted 10 December 2017

Available online 30 December 2017

Keywords:

Rotary heat exchanger

Contact heat transfer

Granular material

Heating plate

Overloaded

ABSTRACT

In the present work, the contact heat transfer between the granular materials and heating plates inside plate rotary heat exchanger (PRHE) was investigated. The heat transfer coefficient is dominated by the contact heat transfer coefficient at hot wall surface of the heating plates and the heat penetration inside the solid bed. A pilot scale PRHE with a diameter of $D_o = 273$ mm and a length of $L = 1000$ mm has been established. Quartz sand with $d_p = 2$ mm was employed as the experimental material. The operational parameters were in the range of $\omega = 1 - 8$ rpm, and $F = 15, 20, 25, 30\%$, and the effect of these parameters on the time-average contact heat transfer coefficient was analyzed. The time-average contact heat transfer coefficient increases with the increase of rotary speed, but decreases with the increase of the filling degree. The measured data of time-average heat transfer coefficients were compared with theoretical calculations from Schlünder's model, a good agreement between the measurements and the model could be achieved, especially at a lower rotary speed and filling degree level. The maximum deviation between the calculated data and the experimental data is approximate 10%.

© 2017 The Authors. Published by Elsevier B.V. This is an open access article under the CC BY-NC-ND license (<http://creativecommons.org/licenses/by-nc-nd/4.0/>).

Introduction

Granular materials are of substantial importance in a variety of industrial processes, such as grain, food products, fertilizer, cosmetics, metallurgy, coal, electronics and other fields. According to the statistics, the processing of granular materials consumes an estimated 10% of the planet's energy budget [1]. Rotary drums are commonly used in above industrial engineering fields, which can be heated directly or indirectly depending on the requirements of production processes, and the working temperature are ranged from 100 to 2000 °C. Most of the rotary drums appear to be cylindrical apparatus with different rotating movement and slope, the granular materials are usually fed at the upper side and flow to the lower end by the rotation of the drum and the force of gravity.

More attentions have been paying on establishing of constitutive equations of granular transport in the rotary drums, several theoretical approaches were confirmed based on the fundamental physics of granular flow and the quantitative relationships were found on mixing and de-mixing, free surface, segregation [2–5]. The internal granular motion is closely relate to the heat transfer phenomenon, and the heat transfer process is a function of certain

operational variables (initial granular temperature, wall temperature, heat transfer coefficient) and granular characteristics (sphericity, cohesiveness, stickiness, specific heat capacity) [6–11].

In our previous work, a new type of plate rotary heat exchanger (PRHE) is developed for granular heating or cooling processes as shown in Fig. 1. This equipment is basically a cylindrical body in which a number of heating plates are arranged symmetrically around the perimeter of the shell. Usually, the cylinder of PRHE is mounted on a set of supporting wheel so that it is sloped under the working condition, helping the transport of granular materials through PRHE. The body of PRHE rotates by the driving of ring gear, providing a tumbling action that continually exposes fresh material to the heating surface. In our previous study, the mean residence time of granular has been investigated experimentally which is illustrated to be one of the most crucial indexes in heat transfer process [12]. Due to its industrial application, the heat transfer between granular materials and heating plates is worthy of studying.

Among the open literatures, the heat transfer to the granular materials in rotating drums has been investigated for a long time [13,14]. Early numerical investigations were carried out to predict heat transfer in rotating drums [15–18]. Fundamental investigations and analytical models were also performed and developed [19–21]. In indirectly heating drums, the contact heat transfer between the covered wall and the solid bed is dominant [22].

* Corresponding authors.

E-mail addresses: xling@njtech.edu.cn (X. Ling), phsight1@hotmail.com (H. Peng).

Nomenclature

A_c	cross section area of contact solid bed [m^2]	n	the total number of granular materials in the plate rotary heat exchanger
A_s	cross section area of solid bed [m^2]	p	pressure [Pa]
A_E	inner cross section area of the plate rotary heat exchanger [m^2]	Q_{total}	total heat transfer of the plate rotary heat exchanger [W]
A_w	contact heat transfer surface between heating plate wall and solid bed [m^2]	Q_{air}	heat transfer between the heating plates and air inside the plate rotary heat exchanger [W]
$c_{p,s}$	specific heat capacity of the solid bed [J/(kg·K)]	Q_s	heat transfer between the heating plates and solid bed [W]
$c_{p,a}$	specific heat capacity of air [J/(kg·K)]	Q_{loss}	heat dissipation of the plate rotary heat exchanger [W]
$c_{p,w}$	specific heat capacity of the heating plate wall [J/(kg·K)]	U	input voltage [V]
D_o	outer diameter of Plate rotary heat exchanger cylinder [mm]	T_m	average temperature of the solid bed [K]
D_i	inner diameter of Plate rotary heat exchanger cylinder [mm]	$T_{s,1}$	temperature of the first granular layer [K]
d_p	average particle diameter [mm]	T_a	air temperature [K]
F	filling degree [%]	T_∞	room temperature [K]
H_s	solid bed height [mm]	R_E	inner radius of the plate rotary heat exchanger [mm]
h	time-average contact heat transfer coefficient [W/(m^2 K)]	R	universal gas constant
h_i	instantaneous transfer coefficient [W/(m^2 K)]	<i>Greek symbols</i>	
h_c	heat transfer coefficient between heating plate wall and the first granular layer [W/(m^2 K)]	τ	time interval of the heating plate sweeping the solid bed [s]
h_g	heat transfer coefficient by penetration in the solid bed [W/(m^2 K)]	τ_c	contact time [s]
h_{wg}	heat transfer coefficient by conduction in the gas gap of the first granular layer [W/(m^2 K)]	θ	filling angle [rad]
h_{2wg}	heat transfer coefficient by conduction in the gas gap of the second granular layer [W/(m^2 K)]	γ	accommodation coefficient
I	input current [A]	σ	modified mean free path of the gas molecules [mm]
L	length of the plate rotary heat exchanger [mm]	λ_a	conductivity of air [W/m K]
m_a	quality of the air inside the plate rotary heat exchanger [kg]	λ_s	conductivity of the solid bed [W/m K]
m_s	quality of the solid bed [kg]	λ_i	conductivity of the insulation material [W/m K]
M	molar mass [kg/kmol]	δ_i	thickness of the insulation
n_c	the number of granular materials in each contact process	ψ	surface coverage factor
		ω	rotary speed [rpm]
		α_i	surface heat dissipation coefficient [W/(m^2 K)]
		φ	void fraction

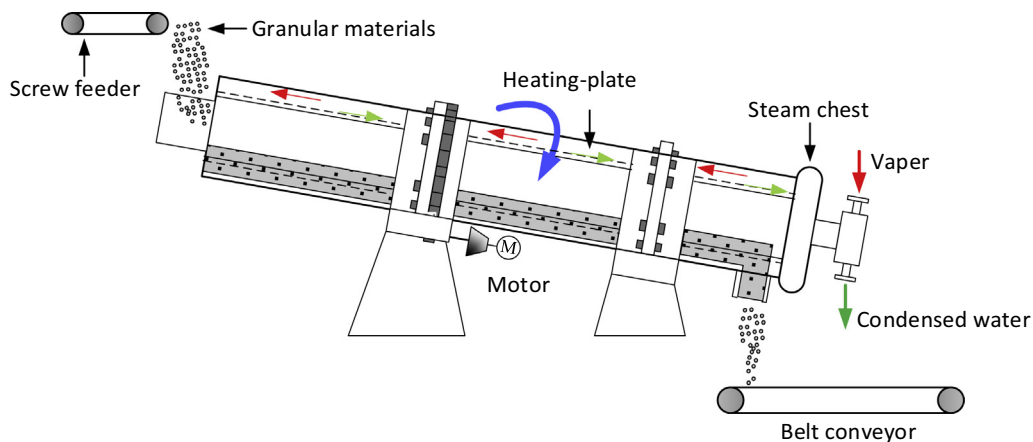


Fig. 1. Schematic of plate rotary heat exchanger.

The experimental investigations carried out by Herz [23–25] revealed that the contact heat transfer coefficient is increasing with the increase of rotating speed, while it is decreasing with the increase of filling degree. Furthermore, the thermos-physical properties of the solid bed such as density, conductivity and heat capacity also showed significant influence on the contact heat transfer coefficient.

As mentioned above, the heat transfer in PRHE strongly depends on the combined transport of mass and heat within the granular materials. The thorough analysis of the heat transfer mechanism in the reverse heat exchanger is not only the improvement of the theory in this field, but also of great significance to the improvement of the equipment application level. For the engineering practice and safe design of PRHE, the contact heat transfer

process should be described as accurately as possible. Accordingly, the heat transfer between the granular materials and heating plates under overloaded condition will be investigated analytically and experimentally. Furthermore, the influence of the operational parameters on contact heat transfer will be studied.

Model of granular heat transfer in PRHE

Heat transfer process

A physical model based on the heat balance is solved through the heating plate wall in order to reach the heat transfer coefficients inside PRHE. The cross section view of the heating plate arrangement and the solid bed inside the PRHE is shown in Fig. 2. The heat carrier (such as steam, hot gas and thermal oil) flows into the inner plate channel side. With the rotation of PRHE, the granular materials are lifted outside and discharged by the heating plates, heat transfer happened between the granular materials and the heat carrier through the contacting of the heating plate wall. The phenomenology of the heat transfer in PRHE is schematically depicted in Fig. 2. The wall of the heating plates, which is made of stainless steel, is heated by the heat carrier inside plate channel.

Q_{total} is the total amount of heat input through the heating plate, and the energy transported to the wall surface is absorbed by the solid bed and the air inside PRHE, a part of the transferred heat is conducted through the shell of PRHE and then proceeds as the heat loss to the surroundings. Based on the heat balance, the total heat transfer of PRHE can be expressed as follows:

$$Q_{total} = Q_{air} + Q_{bed} + Q_{loss} \quad (1)$$

The amount of heat absorbed by the air inside PRHE can be expressed as:

$$Q_{air} = c_{p,a} m_a \frac{dT_a}{dt} \quad (2)$$

And the amount of heat absorbed by the solid bed can be expressed as:

$$Q_{bed} = c_{p,s} m_s \frac{dT_s}{dt} \quad (3)$$

The heat loss from the outer wall of PRHE to the surroundings can be expressed as:

$$Q_{loss} = \frac{(T_m - T_\infty)}{[(D_o + 2\delta_i)/(2\lambda_i) \ln((D_o + 2\delta_i)/D_o) + 1/\alpha_i]} \quad (4)$$

There are two regions in PRHE, free wall surface region and solid bed contact region, which are depend on the filling degree in PRHE, as shown in Fig. 2. The filling degree is defined by the ratio of the solid bed area in the cross section to the total cross section area of PRHE and can be expressed as:

$$F = \frac{A_s}{A_E} \times 100\% = \frac{\frac{\theta}{2} - \sin\frac{\theta}{2} \cos\frac{\theta}{2}}{\pi} \times 100\% \quad (5)$$

where θ can be defined:

$$\theta = 2 \arccos \left(1 - \frac{H_s}{R_E} \right) \quad (6)$$

In the free wall surface region, the heat is conducted from the wall of heating plate to the air inside PRHE. In the solid bed contact region, the heat transfer is controlled by the contact resistance between the heating plate wall surface and the heat penetration inside the solid bed.

Contact heat transfer

The motion of the granular materials inside PRHE is complicated. Therefore, it is necessary for analytical simplicity to assume that: (1) The heat flux of the heating plate wall per unit area is uniformly distributed. (2) The granular materials are well distributed in the solid bed. (3) The granular materials are spherical and the granular sizes distribution is homogeneous. (4) The shape of the granular materials is spherical.

The principle of heat transfer to solid bed from a hot wall surface was proposed by Schlünder [19], which has been widely used in the heat transfer model of packed beds. In Schlünder's work, a thin layer of gas film is assumed to be existed between the granular materials and heating plate wall. The temperature profile in solid bed heated from the hot wall surface is shown in Fig. 3. Near the point of contact between the granular and surface wall, the gas gap is less than the mean free path of the gas molecules. As set forth in [26], the main reason for the contact heat transfer resistance is that the heat conductivity of the gas in the wedge between the granular and surface wall goes to zero when approaching the contact point. Consequently, the conduction and radiation in the gas gap between the heating plate wall and the first layer of granular materials can be considered in accordance with:

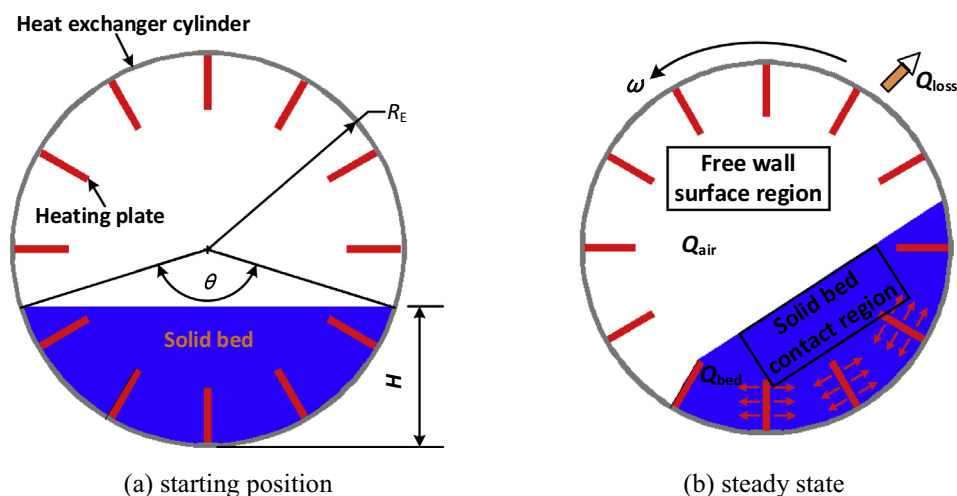


Fig. 2. Schematic cross section of the rotating motion and heat transfer process in PRHE.

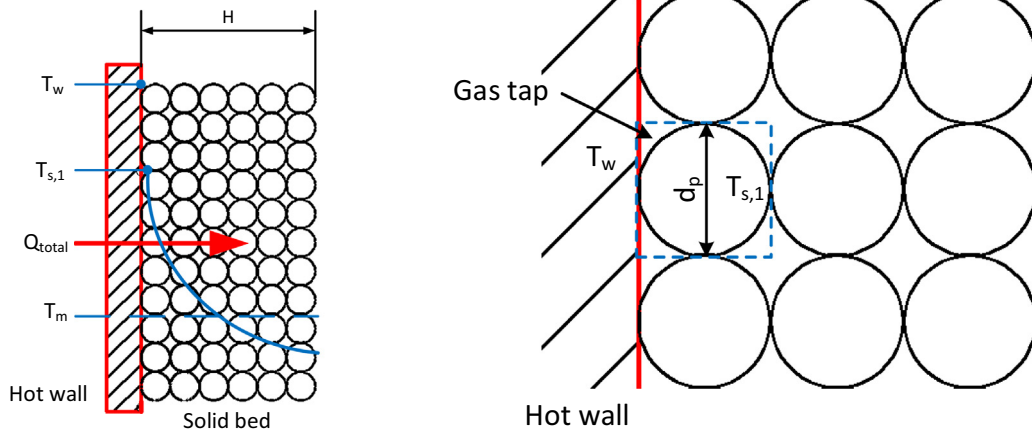


Fig. 3. Temperature profile in a solid bed heated from hot wall [19].

$$h_{wg} = \frac{4\lambda_a}{d_p} \left[\left(1 + \frac{2\sigma}{d_p} \right) \ln \left(1 + \frac{d_g}{2\sigma} \right) - 1 \right] \quad (7)$$

where

$$\sigma = 2 \frac{2 - \Upsilon}{\Upsilon} \sqrt{\frac{2\pi RT_m}{M} \frac{\lambda_a}{p(2c_{p,a} - \frac{R}{M})}} \quad (8)$$

Based on the experimental results [27], the accommodation coefficient is given by the following empirical equation:

$$\lg \left(\frac{1}{\Upsilon} - 1 \right) = 0.6 - \frac{(\frac{1000}{T} + 1)}{2.8} \quad (9)$$

Considering the heat transfer between the heating wall and second layer of granular materials, the contacted heat transfer coefficient between heating wall and granular materials is:

$$h_c = \psi h_{wg} + (1 - \psi) h_{2wg} \quad (10)$$

The granular materials contacting to the heating wall directly is assumed to be arranged in a hexagonal closest packing, and the surface coverage factor $\psi = 0.91$. At each hypothetical static stage, the heat conduction inside the solid bed is expressed by the penetration model [28] as follows:

$$h_p = 2 \sqrt{\frac{\lambda_s \rho_b c_{p,s}}{\pi \tau_c}} \quad (11)$$

Hence, the instantaneous heat transfer coefficient can be obtained:

$$h_i = \frac{1}{\frac{1}{h_c} + \frac{1}{h_p}} \quad (12)$$

Accordingly, the time-averaged heat transfer coefficient can be obtained by integrating during contact time:

$$h = \frac{1}{\tau_c} \int_0^{\tau_c} h_i dt = 2h_c \left(\sqrt{\pi \tau^*} - \ln \left(1 + \sqrt{\pi \tau^*} \right) \right) / (\pi \tau^*) \quad (13)$$

With

$$\tau^* = h_c^2 \tau_c / (\lambda_g \rho_g c_{p,g}) \quad (14)$$

The contact time

For calculating the heat transfer coefficient, it is important to know the contact time between granular materials and heating plates. Under the overloaded condition, the contact time between the granular materials and heating plate is related to the contact

surface of heating plates, diameter of granular materials and the granular coverage factor at any given moment. And the time interval of a single heating plate sweeping the solid bed within a revolution can be calculated as follows:

$$\tau = \frac{\theta}{\pi \cdot \omega} \quad (15)$$

Assuming the material is sufficiently and uniformly contacted with the heating wall, the contact time of a single heating plate within a revolution is calculated by an approximate macro statistic method as proposed below:

$$\tau_c = N \cdot \tau \frac{n_c}{n} \quad (16)$$

It is assumed that the granular materials are uniformly distributed along the axial direction, then, n_c is defined as:

$$n_c = \frac{\phi \cdot A_c}{\frac{\pi}{4} d_p^2} \quad (17)$$

And n is calculated by substituting Eq. (17) to Eq. (16):

$$n = \frac{\phi \cdot A_s \cdot L}{\frac{4\pi}{3} d_p^3} \quad (18)$$

Experiments

Experimental system

The experimental system included following parts: a plate rotary heat exchanger (PRHE), a drive and control unit, an electrical heating & power control unit and a temperature measuring unit. A schematic diagram of the experimental system and the experimental apparatus are shown in Figs. 4 and 5, respectively.

Plate rotary heat exchanger: this unit is basically a cylindrical body which constructed with a seamless stainless steel pipe as the shell of the heat exchanger and has an outer diameter of 273 mm, a total length of 1000 mm and a shell thickness of 4 mm. twelve rectangular plates are arranged uniformly along the circumference as the “heating plates”. One of the rectangular plates is the test heating plate which is used to measure the heat transfer coefficient. The geometric dimension of the test heating plate is 1060 mm × 45 mm × 6 mm, while the effective heating length is 1000 mm. The other rectangular plates are stainless steel plates with the same size of the test heating plate. In order to observe the position of the test heating plate, corresponding mark is arranged on the outer wall of PRHE. At each end of the shell, a

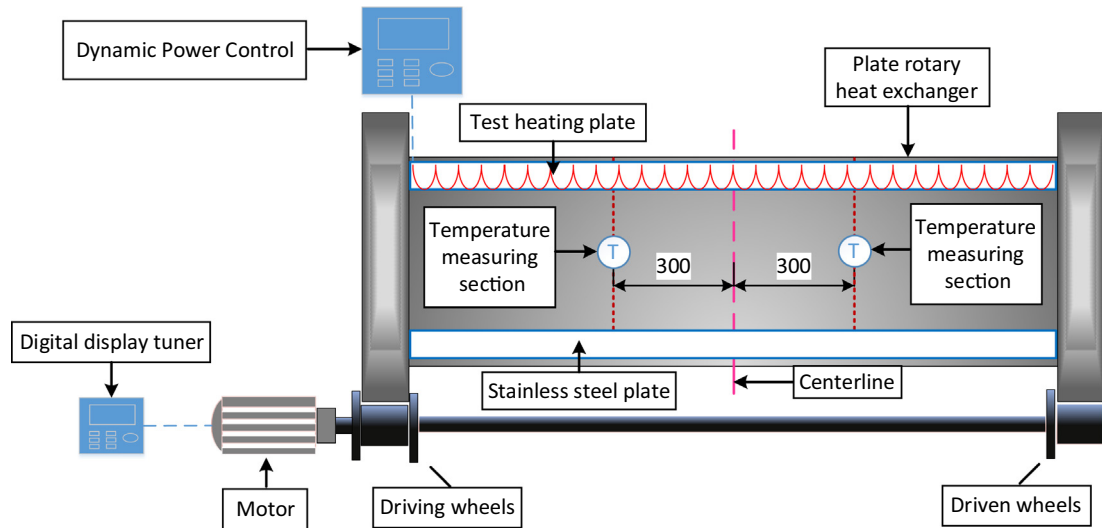


Fig. 4. Schematic of PRHE experimental system.



Fig. 5. Photograph of the experimental apparatus.

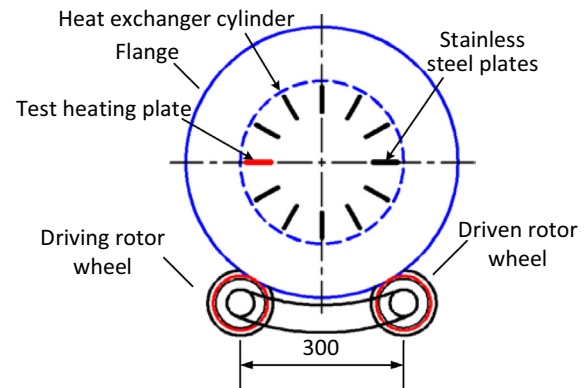


Fig. 6. Cross-sectional representation of the experimental apparatus.

flange is installed as a supporting point. The PRHE body is mounted on the rotor wheels by the contact with the flange.

Drive and control unit: It consists of two pairs of rotor wheels (driving wheels and driven wheels), a stepless speed regulating motor and a digital display tuner. The rotor wheels that working in the style of rolling contact are the important rotating driving components in rotating power transport system. The geometric dimension of both the driving and driven wheels are $\Phi 100 \times 20$ mm, and the separation between the two pairs of rotor wheels are 300 mm, as shown in Fig. 6. The wheels are covered by approximately 10 mm thick rubber layer to prevent slipping between the flange and the wheels. The power is provided by the stepless speed regulating motor, the speed adjustment of PRHE was achieved through the control of motor speed by a digital display tuner. The rotate speed can be regulated at the range of 0 to 30 rpm. The motor provided energy for the driving wheels running, and then the driving wheels led the driven wheels rotating simultaneously through the rubber belt. Due to the action of gravity and friction, PRHE rotated stability.

Electrical heating and power control unit: carbon brush technology is adopted to supply power to the test heating plate continuously and stably. In order to measure and regulate the heating power of the test heating plate, a silicon control, an ammeter and

a voltmeter are arranged on the power line of the test heating plate. Resistance wire is fixed inside the test heating plate to provide a steady heat flow rate during the experimental process.

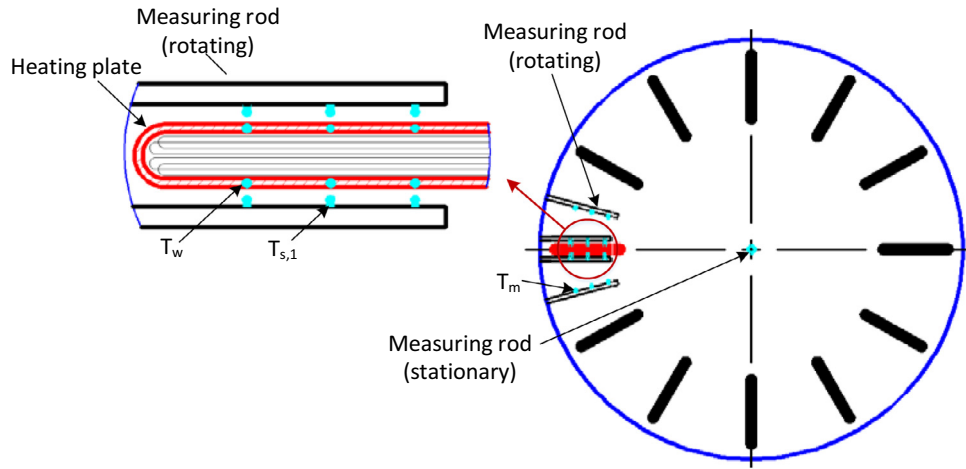
Digital temperature measuring unit: There are two temperature measuring section located about 300 mm from the centerline of PRHE. To draw the temperature profile of the test heating plate surface wall and the solid bed, 12 thermocouples are installed directly at the outer wall surface of the heating plate and 18 thermocouples are fixed on measuring rods at different distance to the inner wall of PRHE cylinder. A fixed measuring rod was positioned stationary at the center of the cross section to assess the delay of the thermocouples. The details of the thermocouples arrangement is presented in Fig. 7. All these thermocouples are K-type with a diameter of 0.5 mm, the temperature data are recorded every five seconds.

Experimental method

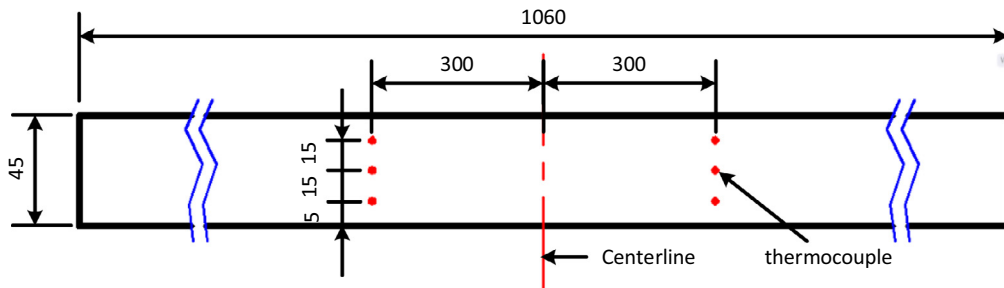
The quartz sand is employed as the granular sample, and the effective thermo physical properties of the solid beds are listed in Table 1, such as average particle size, bulk density, apparent particle density, thermal conductivity and heat capacity.

The experimental procedure is described as follows.

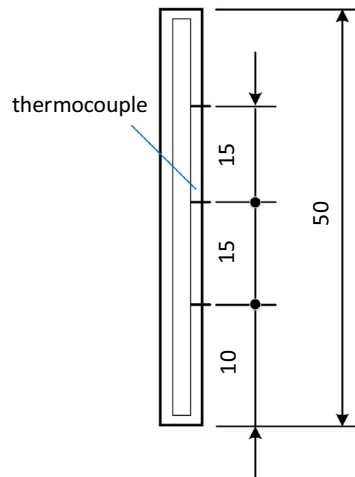
Firstly, the cylinder of PRHE is charged with quartz sands to a filling degree, the total heat capacity of the test heating plate is set to 50 W, which resulting in a feasible maximum wall tempera-



(a) Schematic cross section of the thermocouple arrangement of PRHE



(b) The thermocouple arrangement of the test heating plate



(c) The thermocouple arrangement of the measuring rod

Fig. 7. The thermocouple arrangement for the experimental measurement.

Table 1
The properties of the experimental sample.

Parameter	Unit	Value
d_p	mm	2
ρ_p	kg/m ³	2650
ρ_b	kg/m ³	1390
$c_{p,s}$	J/(kg·K)	1080
λ_s	W/(m·K)	0.518

Table 2
Parameters of experimental conditions.

Parameter	Unit	Value
q	W	50
n	rpm	1, 2, 3, 4, 5, 6, 7, 8
F	(%)	15, 20, 25, 30

ture no higher than 368 K. Then the PRHE is rotated at a predetermined speed according to the experimental conditions listed in Table 2. As soon as the desired wall curve reaches a consistent

tend, it is considered that the experiment has reached a steady state and the temperatures are recorded. At the same time, the location of the test heating plate will be recorded. During the experiment, there has no air passed through PRHE and the heat

transfer at any given moment can be calculated from the heat balance equation:

$$Ul - c_{p,w}m_w \frac{dT_w}{dt} = h_i A_w \cdot (T_w - T_m) \tag{19}$$

During the whole solid bed contact region, the time-average contact heat transfer heat coefficient is acquired by the following formula:

$$h = \frac{1}{\tau_2 - \tau_1} \int_{\tau_1}^{\tau_2} h_i \cdot dt \tag{20}$$

Uncertainty analysis

All the instruments are calibrated before test. The K-type thermocouples have a precision of ±0.1 K, the maximum range of the multimeter is used as the test value, and the accuracy of voltage and is 0.1 V and 0.001A respectively.

The measurement accuracy which is obtained through analysis and estimation of error in experiments is the important basis for evaluating the reliability of experimental data [29,30]. The relative uncertainty analysis is explained according to the theory of error propagation. Consider an indirectly measured variable y, which is a function of several directly measured values and can be determined:

$$y = f(x_1, x_2, x_3 \dots x_n) \tag{21}$$

A total differential of the above function is presented:

$$dy = \sum_{i=1}^n \frac{\partial f}{\partial x_i} dx_i \tag{22}$$

By replacing the corresponding differential variables {dx₁, dx₂ . . . dx_n} with the absolute error of directly measured values {Δx₁, Δx₂, . . . Δx_n} in expression (22), the uncertainty Δy of the indirectly measured variable y can be calculated:

$$\Delta y = \sum_{i=1}^n \frac{\partial f}{\partial x_i} \Delta x_i \tag{23}$$

The uncertainty of the parameters measured in the experiments is listed in Table 3.

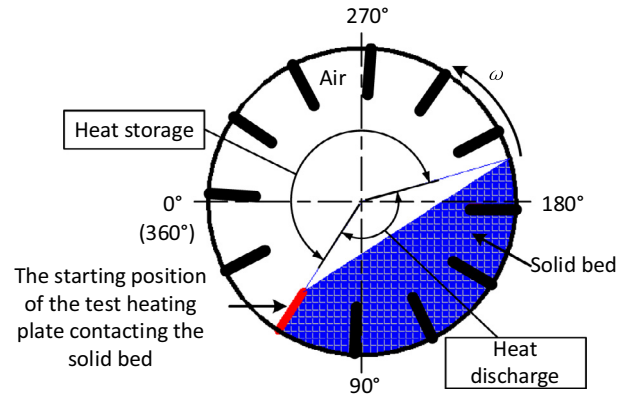
Results and discussions

Unsteady heat transfer characteristics of the heating plate

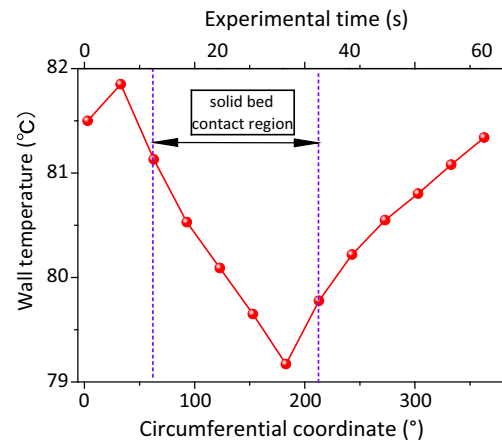
Following the rotation of PRHE, the heating plate is alternately immersed in solid bed contact region and free wall surface region. Due to the difference in physical properties between the granular materials and air inside PRHE, the heat transfer of the heating plate is periodic unsteady. In Fig. 8, the periodic unsteady heat transfer characteristics of the heating plate is presented for Quartz sand, with a constant filling degree of F = 30%, and the rotary speed ω = 1 rpm.

Exemplarily measured the circumferential wall temperature profile of the test heating plate is depicted in Fig. 8(b). It can be

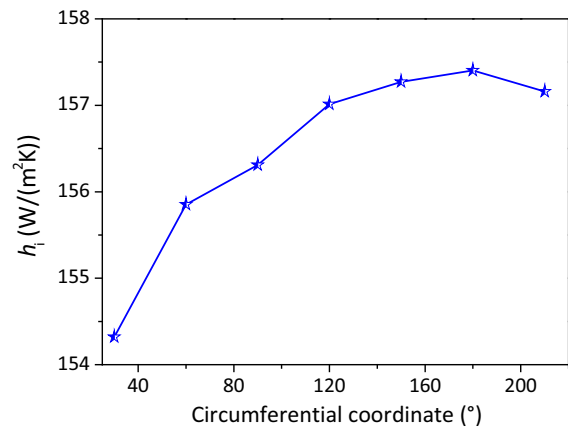
seen that the wall temperature of test heating plate decreases gradually in the solid bed contact region, while in the free wall surface region, the wall temperature is rising gradually. With the change position of the test heating plate, the granular in the solid bed are also in a flowing state. In an immersion revolution, the test heating plate wall is intermittent contact with granular and air, so that the heat transfer process is also instantaneous in time.



(a) The periodic heat transfer process



(b) Circumferential temperature profiles of the test heating plate wall



(c) The instantaneous heat transfer coefficient of the test heating plate at different position

Table 3
Uncertainty analysis of the measured parameters.

Experimental parameters	Unit	Uncertainty of the measurements
<i>l</i>	A	0.33%
<i>U</i>	V	0.26%
<i>T_w</i>	K	0.64%
<i>T_m</i>	K	0.47%
<i>h</i>	W/(m ² K)	3.48%

Fig. 8. The periodic unsteady heat transfer characteristics of the heating plate.

Corresponding to Fig. 8(b), the instantaneous heat transfer coefficient of the test heating plate at different position is shown in Fig. 8(c). With the rotation of PRHE cylinder, the instantaneous change of the heat transfer coefficient in an immersion revolution increases first and then decreases when the test heating plate is about to leave the solid bed. The phenomenon can be attributed to these factors. When the test heating plate has just entered the solid bed, the heat transfer coefficient will gradually increase with the increase of the coverage area of the heating plate wall surface. In addition, under the action of gravity, the granular materials at the bottom is denser than that in the top of solid bed. Thus the gap between the granular materials and heating plate is reduced, which can enhance the heat transfer coefficient. With the rotation of the heating plate, the solid bed is constantly disturbed, which is also beneficial to improve the contact heat transfer coefficient.

As mentioned above, the instantaneous heat transfer coefficient of the test heating plate varies continuously in an immersion revolution. In the subsequent research work, for the purpose of analyze the influence of the experimental factors (rotating speed, filling degree) on the heat transfer coefficient, the measured values of the heating plate instantaneous heat transfer coefficient at different positions are integrated in an immersion revolution as the time-average contact heat transfer coefficient. Meanwhile, the motion and collision of the granular materials are strongly random, the arithmetic mean value of the average heat transfer coefficient of five immersion revolutions is used as the final measured value under each experimental condition.

Influence of rotary speed on time-average contact heat transfer coefficient

In order to discuss the influence of the rotary speed on heat transfer process between test heating plate and solid bed, the experimental investigations are carried out at different rotary speeds with a fixed filling degree. Fig. 9 presents the contours of time-average contact heat transfer coefficient under different rotary speed. According to the figure, the time-average heat transfer coefficient rises faster with the increase of the rotary speed when the rotary speed is relative low. And the contact heat transfer coefficient follows a positive power law with the rotary speed. By fitting the measured data, the indexes are 0.2738, 0.2626 and 0.2617, for the filling degrees at 15%, 20% and 30% respectively. Obviously, increasing the rotary speed of PRHE is beneficial to enhance the contact heat transfer between the granular materials and the heating plate, but the influence is minor in a certain degree of rotary speed. This is because with the rotary speed increases, the heating plate can renew the granular materials faster, both the axial diffusion and mixing strength of the solid bed are improved and finally contributing to enhance thermal conduction inside solid bed. Moreover, the perpendicular velocity component of the granular to the heating plate surface increases by increasing the rotary speed of PRHE, which causes larger contact area and more frequency collision between granular and heating plate, resulting in an improved contact heat transfer. For the sake of particular operation condition, the PRHE is usually worked under a relatively low rotary speed, which causes the minor influence on average heat transfer coefficient.

According to Fig. 9, it can be seen that the variation trend of the calculated contact heat transfer coefficients match the experimental data very well. Under the condition of a fixed filling degree, the calculated data are larger than the experimental measured data, especially at a relatively high rotary speed. That's because in the computational model, the solid bed is assumed to be completely mixed during each contact, actually, there may be some deviation from the experimental conditions.

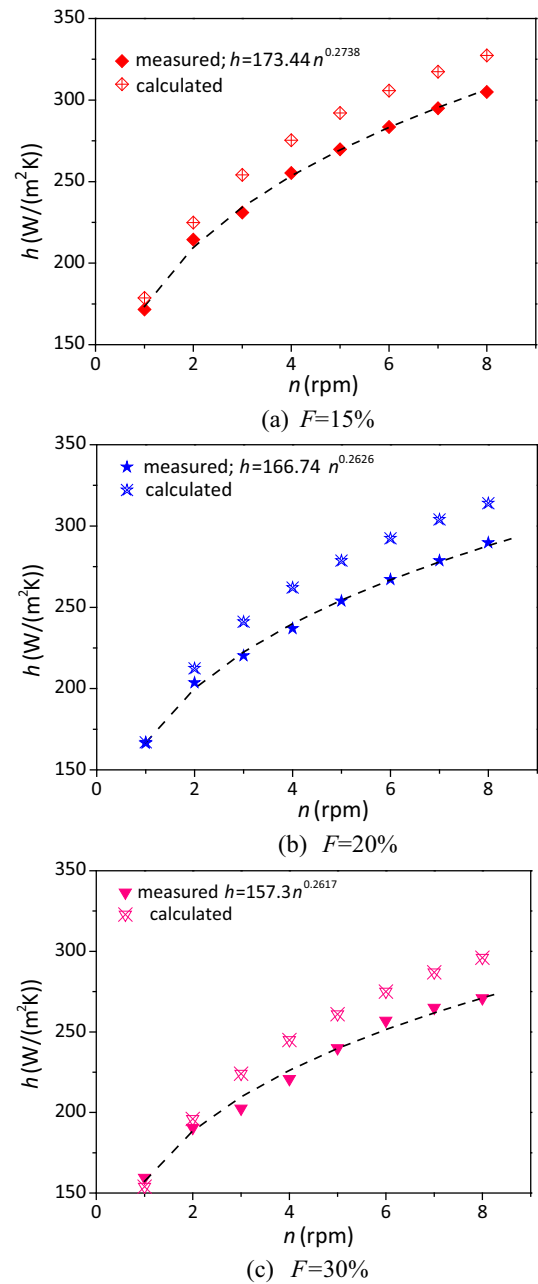


Fig. 9. Comparison of the contact heat transfer coefficient by calculated results and experimental data depended on the rotary speed.

In the interest of analyzing the calculating accuracy, the relative deviation of the calculated data is defined as:

$$\text{relative deviation} = \frac{\text{calculated data} - \text{measured data}}{\text{measured data}} \times 100\% \tag{24}$$

As presented in Fig. 10, The deviations in most of the calculated contact heat transfer coefficients are in the range of 10%. Usually, selection of the heat exchangers is based on the theoretical calculations and enlarges the allowance of 15%~20% in engineering design. The objective is to compensate for the uncertainty caused by the difference between the actual operating conditions and the calculation condition. Therefore, the calculation model can provide a reliable reference for the industrialization design.

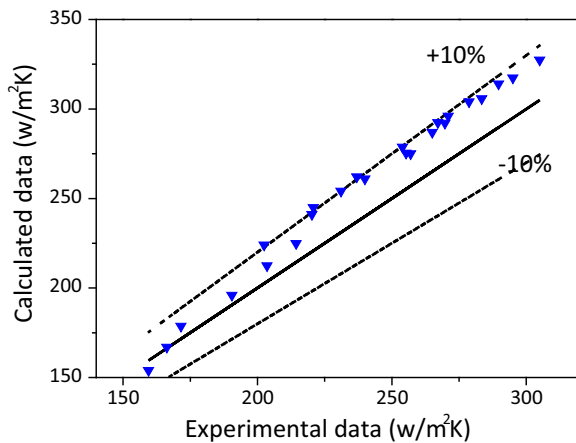


Fig. 10. The relative deviation of the calculated contact heat transfer coefficient.

Influence of filling degree on time-average heat transfer coefficient

Rotary speed and filling degree are two important variables affecting granular-heating plate heat transfer rate. In this section, the experimental data are plotted in a different way, viz. h vs. F . The filling degree is set to 15%, 20%, 25% and 35%. The influence of the filling degree on time-average contact heat transfer coefficient is illustrated in Fig. 11. The experimental data show that the time-average contact heat transfer coefficient is slightly decreased with the increase of filling degree. With the increase of filling degree, the distribution area of the granular inside PRHE increases correspondingly. The larger particle distribution area increases the contact time between the particles and the heating plate, which is the beneficial factor to improve the contact heat transfer coefficient between particles and heating plate. However, on the other hand, the decrease of the number of cycles in the same time interval leads to the decrease of the contact heat transfer coefficient due to the increase of the single cycle time of the granular motion. Moreover, granular materials can eventually reach well mixed states for low filling degree levels [31], and in our previously research work [32], it is indicated that the solid bed temperature reaches thermal uniformity faster under lower filling degree condition, for the granular materials can be mixed more entirely per unit of time, and faster mixing causes rapid heat transfer from heating plate surface wall to solid bed. Qualitatively, the same effect was also reproduced by Schlünder and Mollekopf [19].

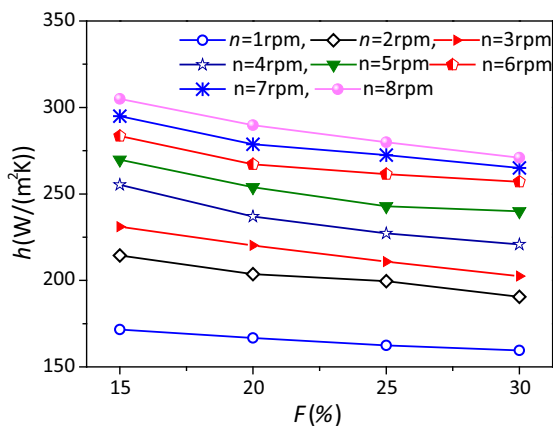


Fig. 11. Comparison of the contact heat transfer coefficient depended on the filling degree.

Conclusion

In this paper, contact heat transfer between granular materials and heating plates inside PRHE was investigated theoretically and experimentally. The theoretical prediction of the contact heat transfer coefficient was presented based on Schlünder's model. The influences of the operational parameters on contact heat transfer coefficient were presented, and the experimental data were compared with the calculated data. The main conclusions are drawn as follows:

- (1) The heat transfer inside PRHE is controlled by the contact heat transfer coefficient at hot wall surface of the heating plates and the heat penetration inside the solid bed.
- (2) With the rotation of PRHE, the heat transfer of the heating plate is periodic unsteady. During an immersion revolution, the wall temperature of test heating plate decrease gradually in the solid bed contact region. While in the free wall surface region, the wall temperature is rising gradually.
- (3) The variable of time-average contact heat transfer coefficient follows a positive power law with rotary speed. The time-average contact heat transfer coefficient increases with the increase of rotary speed, especially when the rotary speed is relatively low.
- (4) The time-average contact heat transfer coefficient decreases approximately linearly with the increase of the filling degree.
- (5) The variation trend of the calculated contact heat transfer coefficients matches the experimental data very well, and the maximum deviation between the calculated data and the experimental data is 10%. Therefore, the calculation model can provide a reliable reference for the industrialization design.

Acknowledgement

The authors acknowledge the financial support provided by funds of the program of National Natural Science Foundation of China (Grant no. 51576095), Natural Science Foundation of Jiangsu Province (Grant No. BK20151539) and Ocean Engineering Equipment Research Project of Ministry of Industry and Information Technology (MIIT [2014]505).

References

- [1] Mullin T. Mixing and de-mixing. *Science* 2002;295(5561): 1851–1851.
- [2] Grajales LM, Xavier NM, Henrique JP, et al. Mixing and motion of rice particles in a rotating drum. *Powder Technol* 2012;222(5):167–75.
- [3] Maoqiang Jiang, Yongzhi, et al. Enhancing mixing of particles by baffles in a rotating drum mixer. *Particuology* 2011;09(3):270–8.
- [4] Ottino JM, Lueptow RM. On mixing and demixing. *Science* 2008;319(5865):912–3.
- [5] Umbanhowar PB, Lueptow RM, Ottino JM. Modeling granular materials: A test bed for framing and analysis. *Aiche J* 2013;59(59):3237–46.
- [6] Nan G, Jie Y, Xu W, et al. DEM simulation and analysis of particle mixing and heat conduction in a rotating drum. *Chem Eng Sci* 2013;97(7):225–34.
- [7] Xiao YL, Specht E. Temperature distribution within the moving bed of rotary kilns: measurement and analysis. *Chem Eng Process Process Intensif* 2010;49(2):147–50.
- [8] Fiers B, Ferschneider G, Maillat D. Reduced model for characterization of solid wall effects for transient thermal dispersion in granular porous media. *Int J Heat Mass Transf* 2010;53(25–26):5962–75.
- [9] Cook CA, Cundy VA. Heat transfer between a rotating cylinder and a moist granular bed. *Int J Heat Mass Transfer* 1995;38(3):419–32.
- [10] Figueroa I, Vargas WL, McCarthy JJ. Mixing and heat conduction in rotating tumblers. *Chem Eng Sci* 2010;65(2):1045–54.
- [11] Chaudhuri B, Muzzio FJ, Tomassone MS. Experimental validated computations of heat transfer in granular materials in rotary calciners. *Powder Technol* 2010;198(1):6–15.

- [12] Duan L, Cao Z, Yao G, Ling X, Peng H. Visual experimental study on residence time of particle in plate rotary heat exchanger. *Appl Therm Eng* 2017;111:213–22.
- [13] Saeman WC, Mitchell TR. Analysis of rotary dryer and cooler performance. *Chem Eng Prog* 1954;50(9):467–75.
- [14] Wes GWJ, Drinkenburg AAH, Stemerding S. Heat transfer in a horizontal rotary drum reactor. *Powder Technol* 1976;13(2):185–92.
- [15] Cribb JL, Langley PA, Sass A. Simulation of the heat transfer phenomena in a rotary kiln. *Ind Eng Chem Process Des Dev* 1969;8(4): 597–597.
- [16] Liu XY, Zhang J, Specht E, et al. Analytical solution for the axial solid transport in rotary kilns. *Chem Eng Sci* 2009;64(2):428–31.
- [17] Komossa H, Wirtz S, Scherer V, et al. Transversal bed motion in rotating drums using spherical particles: comparison of experiments with DEM simulations. *Powder Technol* 2014;264(3):96–104.
- [18] Zhou JH, Yu AB, Horio M. Finite element modeling of the transient heat conduction between colliding particles. *Chem Eng J* 2008;139(3):510–6.
- [19] Schlünder EU. Heat transfer to packed and stirred beds from the surface of immersed bodies. *Chem Eng Process* 1984;18(1):31–53.
- [20] Yagi S, Kunii D. Studies on effective thermal conductivities in packed beds. *AIChE* 1957;3:373–81.
- [21] Vargas WL, McCarthy JJ. Heat conduction in granular materials. *AIChE* 2001;47:1052–9.
- [22] Herz F, Mitov I, Specht E, et al. Influence of operational parameters and material properties on the contact heat transfer in rotary kilns. *Int J Heat Mass Transfer* 2012;55(25–26):7941–8.
- [23] Herz F, Mitov I, Specht E, et al. Experimental study of the contact heat transfer coefficient between the covered wall and solid bed in rotary drums. *Chem Eng Sci* 2012;82(1):312–8.
- [24] Nafsun AI, Herz F, Specht E, et al. The contact heat transfer in rotary drums in dependence on the particle size ratio. *Begel House Inc*; 2014.
- [25] Nafsun AI, Herz F, Specht E, et al. Experimental investigation of thermal bed mixing in rotary drums. In: *International conference on heat transfer, fluid mechanics and thermodynamics*; 2015.
- [26] Schlünder EU, Mollekopf N. Vacuum contact drying of free flowing mechanically agitated particulate material. *Chem Eng Process Intensif* 1984;18(2):93–111.
- [27] Schlünder DIEU. Wärmeübergang an bewegte Kugelschüttungen bei kurzfristigem Kontakt. *Chem Eng Technol* 1971;43(11):651–4.
- [28] Lybaert P. Wall-particles heat transfer in rotating heat exchangers. *Int J Heat Mass Transfer* 1987;30(8):1663–72.
- [29] Rabinovich SG. *Measurement errors and uncertainties*. New York: Springer; 2005.
- [30] Qian Zheng, Wang Zhongyu, Liu Guili. *Analysis of measurement deviation and data processing*. Beihang University Press; 2008.
- [31] Liu PY, Yang RY, Yu AB. DEM study of the transverse mixing of wet particles in rotating drums. *Chem Eng Sci* 2013;86(5):99–107.
- [32] Li M, Ling X, Peng H, et al. An investigation on heat transfer of granular materials in the novel flighted rotary drum. *Can J Chem Eng* 2016.